Separation of Gelation From Vitrification in Curing of a Fiber-Reinforced Epoxy Composite

BRYAN BILYEU *and* WITOLD BROSTOW

Laboratory of Advanced Polymers and Optimized Materials (LAPOM)
Department of Materials Science
University of North Texas
P.O. Box 305310
Denton, TX 76203-5310

and

KEVIN P. MENARD

Perkin Elmer Instruments
761 Main Ave. F71
Norwalk, CT 06987

Prepregs of a mixture of the tetrafunctional epoxy tetraglycidyl 4,4-diaminodiphenyl methane (TGDDM) and the tetrafunctional amine 4,4'-diaminodiphenylsulfone (DDS) were characterized with temperature-modulated DSC (TMDSC) as well as dynamic mechanical analysis (DMA). The baseline shift of the glass transition was separated from the curing exotherm by using temperature-modulated and step scan DSC temperature scans. Likewise, the baseline shift in heat capacity due to vitrification was isolated using TMDSC isotherms. Using the TMDSC glass transition temperature, degree of conversion, and vitrification results, combined with the gelation data generated from DMA, a time-temperature-transformation (TTT) diagram was constructed, providing information necessary for optimization of industrial processing of the epoxy prepreg. Thus, effects of storage, preprocessing, and postprocessing on the overall curing process are taken into account.

1. INTRODUCTION

Fiber-reinforced epoxy prepregs are commonly processed using isothermal curing. Although processing appears simple, the development of properties during curing is a complex multistep process. In addition, the relationship between the curing temperature and time to a specific conversion value is not linear. Industrial processing control is simplified using a time-temperature-transformation (TTT) diagram. However, construction of such a TTT diagram requires knowledge of the rate and degree of conversion as well as the time to reach gelation and vitrification at each isotherm. The rate and degree of conversion is determined either with a series of DSC isotherms, which show the change of enthalpy in time or with the change in the glass transition temperature T_g during the isothermal cure. Accuracy and resolution of T_g measurements by DSC are improved by using heat capacity C_p rather than enthalpy. Since gelation appears as a change in physical properties, it is conveniently determined by DMA. Vitrification as a rubber to glass transition appears in both DMA and DSC. Although vitrification is commonly determined by DMA, DSC offers increased temperature accuracy and control. However, since vitrification occurs before complete conversion, the T_g is usually masked by the curing exotherm in traditional DSC. Since vitrification and curing are thermodynamically different effects, one should be able to separate the two signals by using either temperature modulated DSC (TMDSC) or step scan DSC.

2. EPOXY CURE CHARACTERIZATION: OPTIONS

To obtain the most useful and reliable characterization of the curing process we need to consider in turn the options available. Characterization of the epoxy curing reaction and generation of a TTT diagram requires

knowledge of the rate and degree of cure as a function of time and temperature as well as the conditions which produce gelation, vitrification, full cure and degradation. The rate and degree of cure is typically tracked by a change in a cure-dependent property, such as the glass transition temperature T_g. Gelation can be determined by examining the molecular weight-dependent properties. Since vitrification is a rubber-to-glass transition, it results in a thermodynamic as well as a physical change. A detailed review of thermal analysis techniques applicable to epoxy characterization is available (1) as well as an extensive study using a variety of techniques to fully characterize an epoxy system (2).

Many thermosetting polymer systems exhibit a relationship between the T_g and the degree of chemical conversion. Most epoxy-amine systems exhibit a linear relationship, which implies that the change in molecular structure with conversion is independent of the cure temperature (3).

The most convenient and generally most accurate method for determining the T_g of polymers is differential scanning calorimetry (DSC). The T_g is taken as the temperature at the inflection point (peak of derivative curve) of the baseline shift in heat flow or as the temperature at the half height shift in baseline heat flow. The shift in baseline heat flow associated with the glass transition is a result of the difference in heat capacity between the rubber and the glass. Since this shift is an effect of the heat capacity change, *resolution of the glass transition can be increased* by calculating and plotting the constant pressure heat capacity, C_p.

The versatility of DSC to measure both exotherms and T_gs is also a limitation; when measuring an uncured or a partially cured thermoset, a residual exotherm follows the T_g being measured, sometimes even overlapping. Accurate T_g calculations require stable baselines before and after the transition and the curing exotherm interferes with the upper baseline. In these cases, the T_g can only be determined as the onset.

One alternative to the measurement of C_p is temperature-modulated DSC (TMDSC). TMDSC utilizes a modulated temperature ramp. The basis for the modulation signals and evaluation, including the phase lag, is derived from electrical signal modulation in the electronics and telecommunications field. Analogous to dynamic mechanical analysis (DMA), TMDSC mathematically deconvolutes the response into two types of signals, an in-phase and an out-of-phase response to the modulations, as well as producing an average heat flow.

A Fourier transform deconvolutes the signal to produce an average heating rate (q_{av}), an average heat flow (h_{av}), an amplitude of heating rate (A_q), an amplitude of heat flow (A_h) and a phase angle between the heating rate and heat flow (φ)(4). Schawe's technique (5–7) uses a linear response approach, which begins with the total heat capacity ($C_p^T = h_{av}/q_{av}$) and includes a C_p value calculated as the ratio of the heat flow amplitude to the heating rate amplitude, the complex heat capacity ($C_p^* = A_h/A_q$). The complex heat capacity (C_p^*) is separated into two components, real and imaginary:

$$C_p^* = C_p' + iC_p'' \quad (1)$$

with C_p' representing the real, in-phase component, termed storage heat capacity, and C_p'' representing the imaginary, out-of-phase component, termed loss heat capacity. The two values are calculated using the phase angle, φ, between the signal and response:

$$C_p' = C_p^* \cos\varphi \quad (2)$$

$$C_p'' = C_p^* \sin\varphi \quad (4)$$

As in DMA measurements, the storage signal will include the elastic or in-phase response of the material, which in this case represent the molecular level responses, including glass transitions and melting. The loss signal represents viscous or out-of-phase events, which are the kinetic effects, such as stress relaxation and curing. The total heat capacity is the non-separated average signal, which is equivalent to the heat capacity signal produced by traditional DSC. In epoxy T_g shifts, this allows separation of the T_g from the exotherm.

Gelation represents a change in mechanical properties, but typically not a change in conversion rate. Thus, gelation does not appear in calorimetric measurements. However, as already pointed out by one of us (8), it does appear prominently in DMA.

Although vitrification is a thermal transition from a rubber to a glass and does appear in DSC measurements (9), the determination of the point and quantification of the shift in baseline heat flow or C_p usually occurs around the end of the curing and as such is usually masked by the curing reaction exotherm. This is one of the clearest applications of TMDSC since the curing exotherm appears in the loss C_p and the vitrification appears in the storage C_p (10–12).

The first epoxy TTT diagram, proposed by Gillham and Enns (13), was constructed from torsional braid analysis (TBA), a torsional DMA measurement. DMA has been used extensively to investigate the vitrification point, and continues to be the most common method. However, as determined earlier by one of us (14), DMA produces higher T_g values than DSC because of the measurement of extrinsic mechanical properties rather than intrinsic heat capacity and the poorer temperature control of the instrument. DSC could produce more accurate and meaningful T_g and vitrification points—if these transitions were separated from the curing exotherm. Thus, we turn to TMDSC. Can TMDSC isolate the T_g and vitrification points?

In other words, on one hand we have several aspects of curing that all must be determined. On the other hand, we have several techniques at our disposal. We need to define a combination of techniques that

will provide sufficient, reliable and if possible fast characterization of the curing process.

3. EXPERIMENTAL

Hercules (Hexcel) 8552 neat resin and glass fiber-reinforced prepregs, which are a mixture of the tetrafunctional epoxy tetraglycidyl 4,4-diaminodiphenyl methane (TGDDM) and the tetrafunctional amine 4,4'-diaminodiphenylsulfone (DDS), along with an ionic initiator/accelerator and a thermoplastic modifier were studied. The fiber-reinforced prepregs contain 66 weight percent unidirectional glass fiber.

DSC, TMDSC and Step Scan DSC experiments were performed on a Perkin-Elmer Pyris-1 DSC equipped with liquid nitrogen cooling, operating on a Windows NT platform. For comparison, DSC experiments were also performed on a Perkin-Elmer DSC-7 with ice coolant, operating on a UNIX platform. Both DSCs were calibrated for temperature and heat of fusion with indium as the standard, following ASTM procedures.

TMDSC scans were performed in two modes—Heat/Cool and IsoScan. Heat Cool runs are a 10°C heating at 20°C/min, followed by a 5°C cooling at 10°C/min, for the average heating rate of 5°C/min. IsoScan runs were a 30 second isotherm followed by a 5°C heating at 10°C/min, which also yields the average rate of 5°C/min. T_g values were calculated as the half height shift in baseline storage C_p. Exothermal changes in enthalphy in the loss C_p were determined by comparing the area under the curve to the total. Isothermal TMDSC determination of vitrification point experiments were performed in Heat/Cool mode, heating to 5°C above the isothermal temperature at 10°C/min. and cooling to 5°C below at 10°C/min. The vitrification point was calculated as the half height shift in baseline storage C_p just as traditional glass transitions are located.

StepScan DSC scans involve two steps: heating and isothermal. The scans were a 5°C increase at 10°C/min. followed by a 30 second isotherm, repeated cyclically. From this, a separated C_p curve was generated. T_g and vitrification could be separated from the curing exotherm.

DMA experiments were performed in both 3-point bending and parallel plate compression, carried out on a Perkin-Elmer DMA-7e using liquid nitrogen cooling for scans and ice for isotherms, operating on a Windows NT platform. The DMA-7e was calibrated for temperature using indium following ASTM E1867-97 and for height using a quartz standard. The 3-point bending apparatus used on the 0.55 mm thick prepreg tapes was a 5 mm wide probe with 5 mm separation between supports. The bending program used 10 μm amplitude in position control. The parallel plate compression measurements were performed on 0.55 mm thick prepreg tapes using a 5 mm diameter circular plate in a 10 μm amplitude position control. DMA temperature scans were performed in both modes to determine the gelation temperature, as well as the initial and final T_gs.

4. GLASS TRANSITION TEMPERATURES

The T_g shift in time for specific isothermal curing temperatures was determined by TMDSC (*Fig. 1*), Step Scan DSC (*Fig. 2*), standard DSC and DMA. TMDSC and Step Scan DSC produces similar values of glass transition temperature as a function of curing time and temperature. We chose to use TMDSC rather than Step Scan DSC because TMDSC was also used for the pseudo-isothermal measurements of vitrification. These values were consistent with standard DSC and lower than DMA results. However, the DSC values were only measurable as onset values because of the overlap of the curing exotherm. The DMA values were consistently higher because we were measuring the mechanical properties that are results of the glass transition rather than the actual change in internal specific heat.

The TMDSC values were tabulated and the shift for various isotherms are plotted as a function of time in *Fig. 3*. The curves demonstrate an increase in the rate and higher final T_g for higher curing temperatures. Using a logarithmic scale, a linear plot is generated in *Fig. 4*. This linear plot is used to determine the shift factor between different curing temperatures.

While the TMDSC measurements were used for the shift calculation, we note that the step change in heat capacity did decrease with increasing degree of cure owing to the high crosslink density.

5. GEL POINTS

The gel point was measured as the peak in tangent delta from parallel plate DMA measurements, as shown in a 160°C isotherm in *Fig. 5* and a series of different isotherms in *Fig. 6*. Gelation was also seen as a poorly resolved peak in the 3-point bending DMA measurements shown in *Fig. 7* for a 160°C isotherm; it occurred at comparable values, but clearly parallel plate is the technique we recommend.

6. VITRIFICATION

Vitrification was determined using TMDSC and DMA in both 3-point bending and parallel plate modes. Using TMDSC, vitrification was determined as the baseline shift in isothermal TMDSC measurements, as seen in the series in *Fig. 8*.

For comparison, vitrification was also measured by 3-point bending DMA experiments. The resulting tangent delta curves for a series of isotherms are shown in *Fig. 9*. Vitrification also appeared in the parallel plate DMA measurements shown earlier in *Fig. 5* as poorly resolved peaks.

As expected, the DMA vitrification times were consistently higher for all isotherms because of the measurement of extrinsic properties rather than the intrinsic heat capacity of the TMDSC. The larger sample size and the temperature control system means that the accuracy of transition temperatures are much lower than DSC, TMDSC in particular. Thus, we have

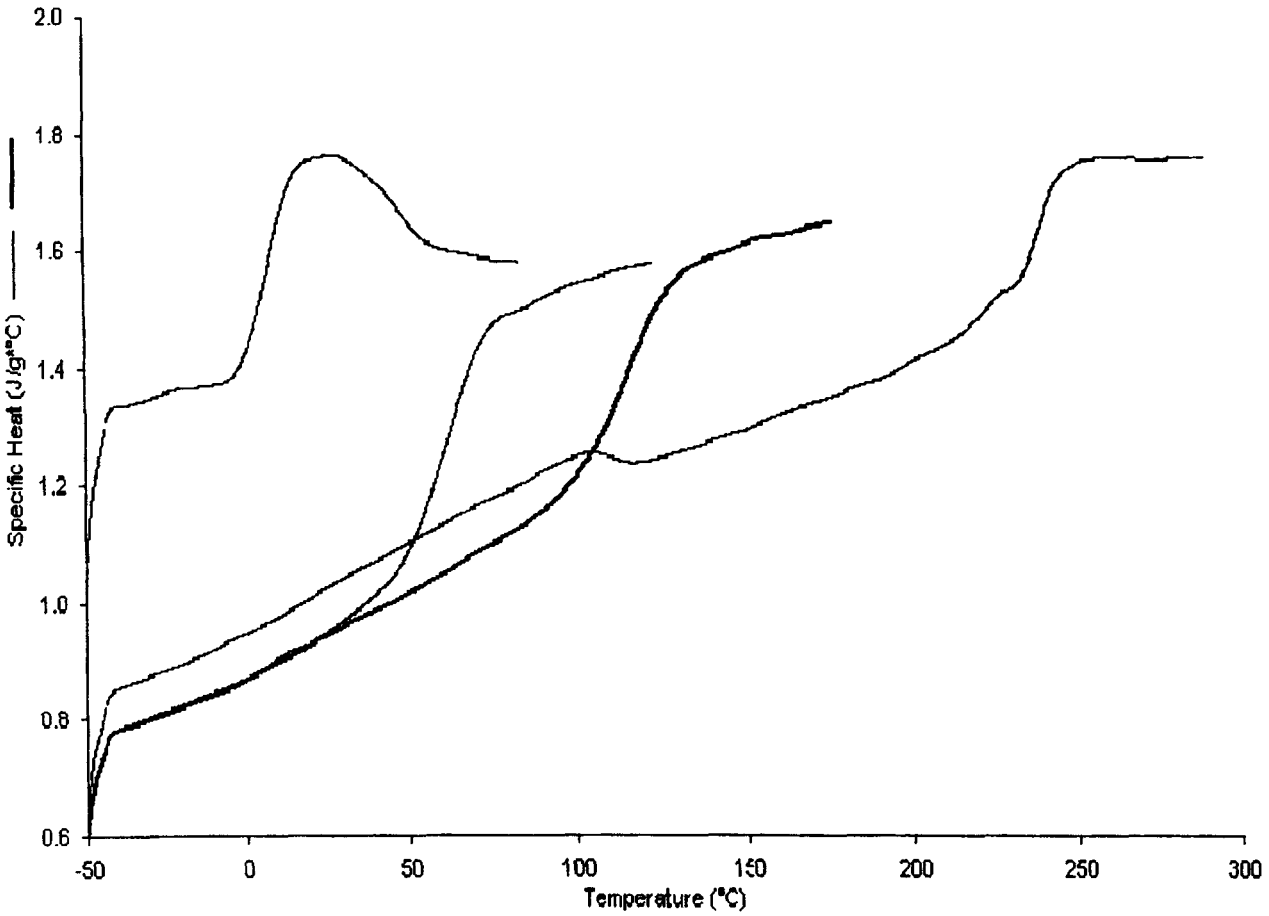

Fig. 1. Changes in T_g as a function of the degree of cure, as seen in the storage heat capacities of separated TMDSC scans.

an answer to one of the questions asked at the end of Section 2. We recommend TMDSC as the technique of choice for the determination of vitrification.

7. THE TTT DIAGRAM

A time-temperature-transformation (TTT) diagram (*Fig. 10*) was constructed from the best resolved gelation and vitrification data. The initial T_g was determined by TMDSC with DMA 3-point bending included for comparison. The final T_g was measured by TMDSC and DMA 3-point bending. The DMA are the best resolved, due to the high filler content. The increase in T_g with time at various temperatures was measured by TMDSC. Gelation was measured by DMA parallel plate while vitrification was measured by TMDSC. The regions and transitions identified follow conventions proposed by Gillham.

At temperatures below the T_{g0} (6°C) there is no reaction, so this is the safe storage temperature. Between T_{g0} and $T_{g\text{-}gel}$ (6 to 86°C) the material will react, albeit very slowly, and will eventually vitrify before it gels. Between $T_{g\text{-}gel}$ and $T_{g\text{-}vit}$ (86 to 248°C) the material will first gel, then vitrify. Above $T_{g\text{-}vit}$ (248°C) the material will gel, but will not vitrify. This diagram provides an easy-to-read description of the transformations taking place in processing of composite prepregs and allows manipulation of processing conditions to modify physical properties toward desired ranges of values.

8. CONCLUDING REMARKS

In summary, TMDSC and step scan DSC provide improved accuracy over common DMA in T_g and vitrification measurements without the overlap of the curing exotherm in traditional DSC. This is due to improved temperature control, small sample size and the measurement of heat capacity rather than mechanical properties. Gelation should be measured by DMA since it involves molecular weight and crosslink density effects. This combination of techniques provides the information necessary for a TTT diagram which characterizes an epoxy system.

In this paper we have studied a commercial epoxy. We are also working on chemical epoxy modification (15–17). We intend to verify in the future whether the modified epoxies lend themselves to the same approach—including the development of TTT diagrams.

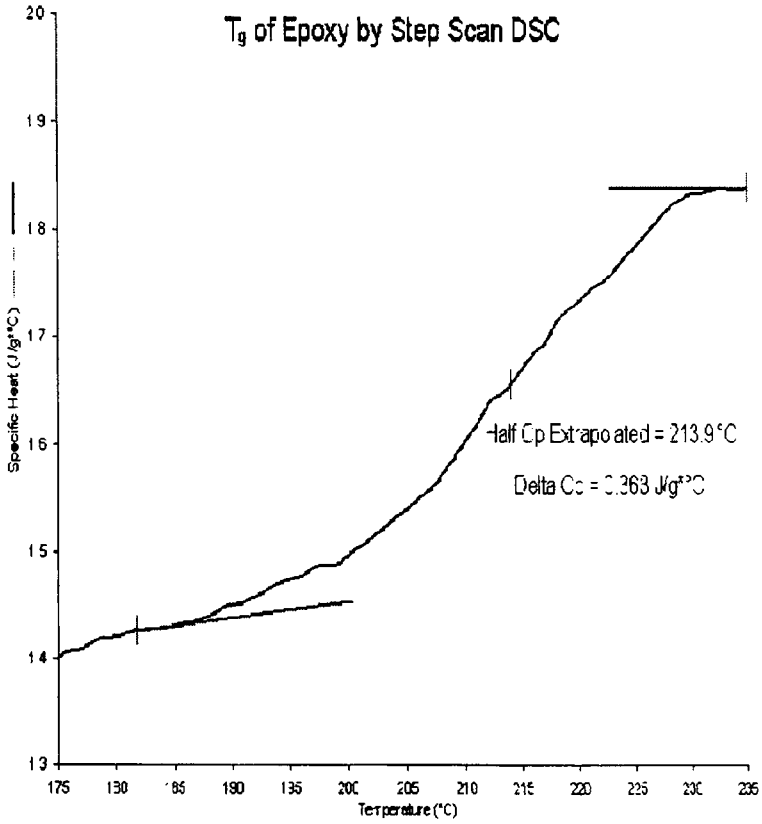

Fig. 2. Step Scan DSC temperature scan with the T_g identified and the curing exotherm eliminated.

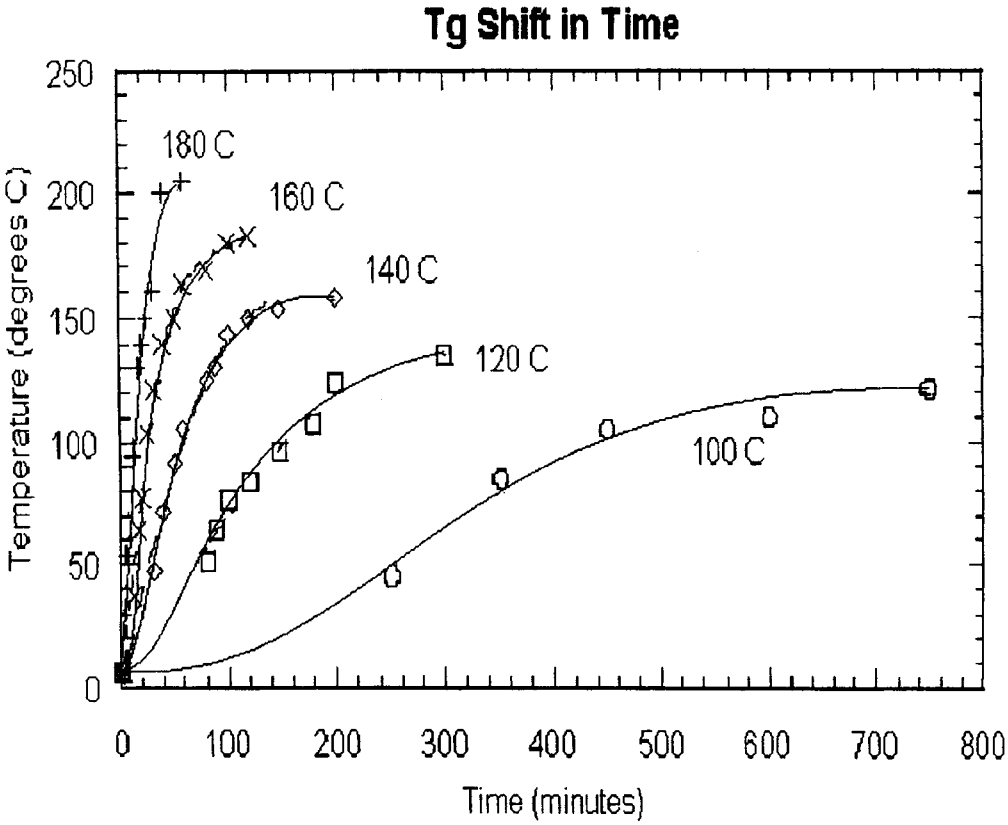

Fig. 3. Shift in T_g in time for isothermal cure diagrams.

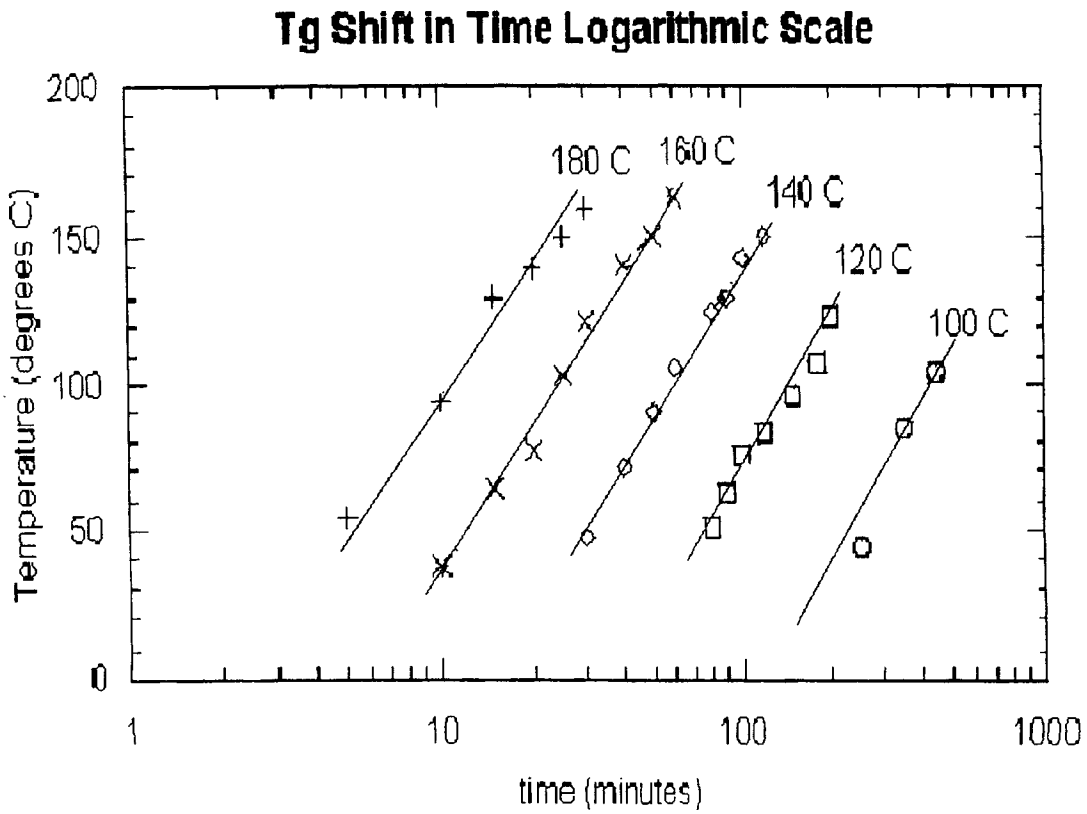

Fig. 4. Shift in T_g in time for isothermal cure temperatures on the logarithmic scale.

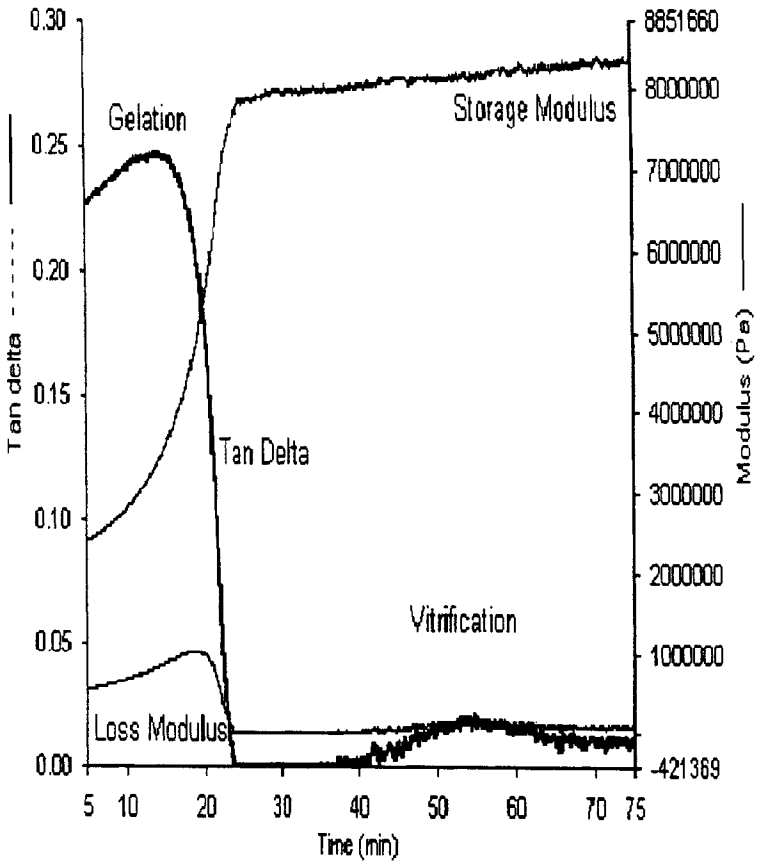

Fig. 5. A parallel plate DMA isotherm at 160°C showing peak in tangent delta at gelation.

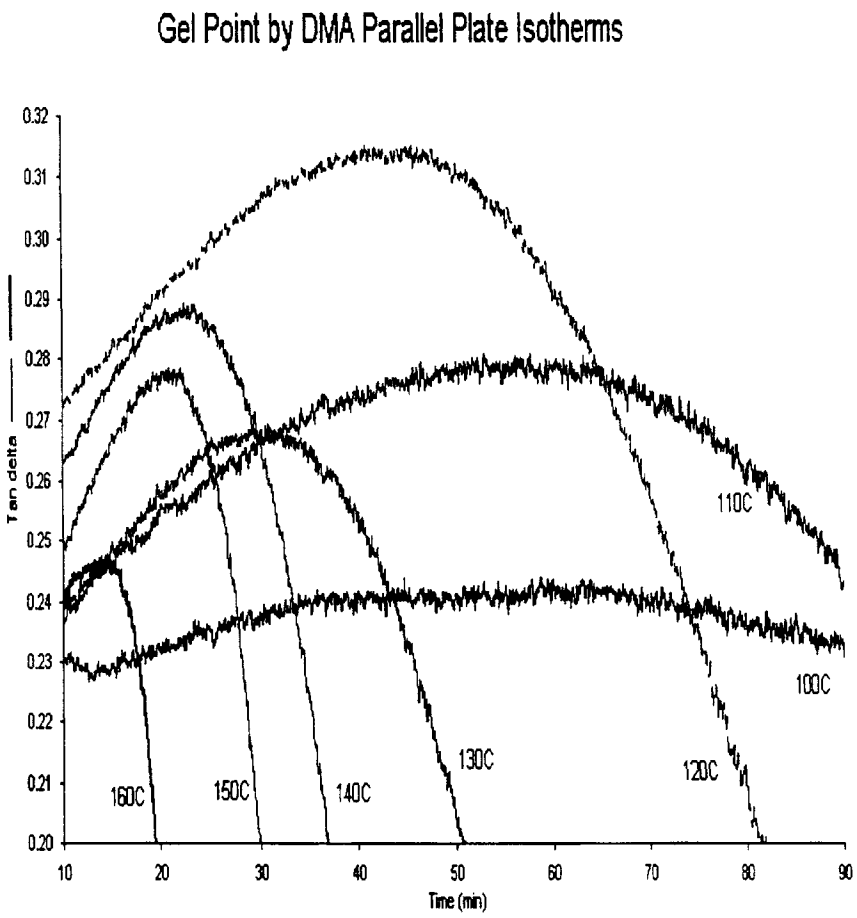

Fig. 6. A series of parallel plate DMA isotherms showing the shift in time to gelation for different temperatures.

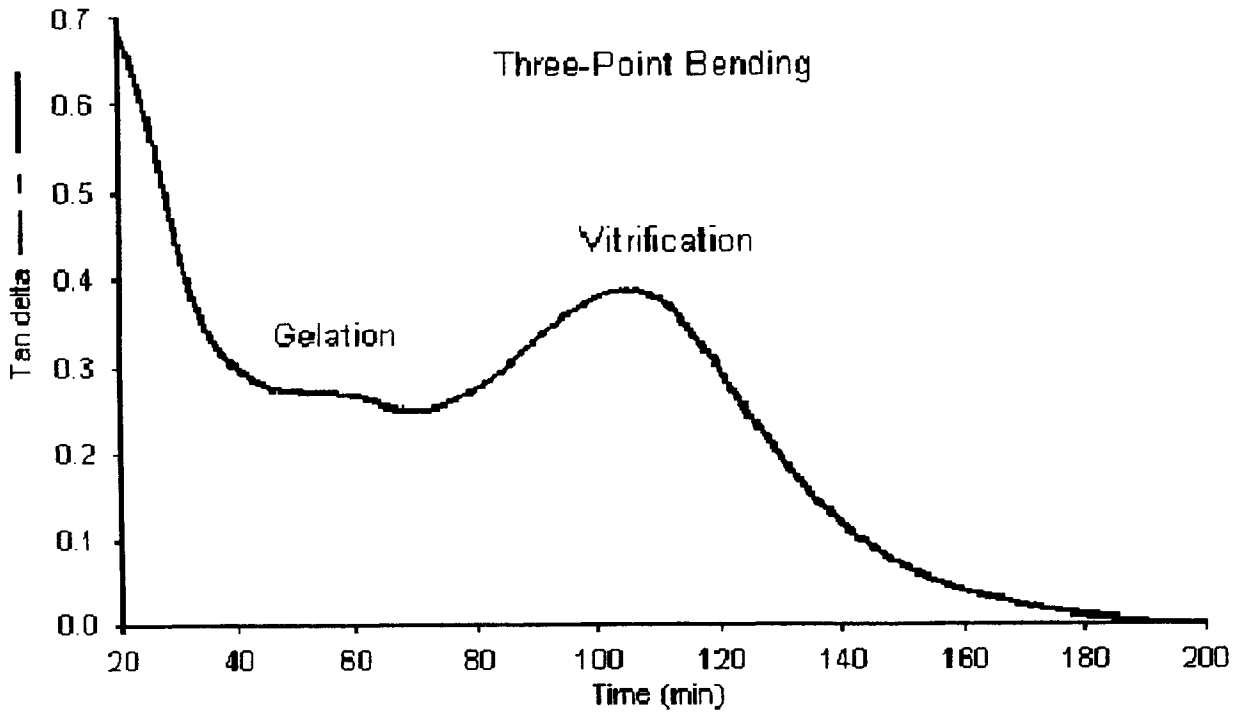

Fig. 7. A 3-point bending DMA isotherm at 160°C showing gelation as a poorly resolved peak before the defined vitrification peak.

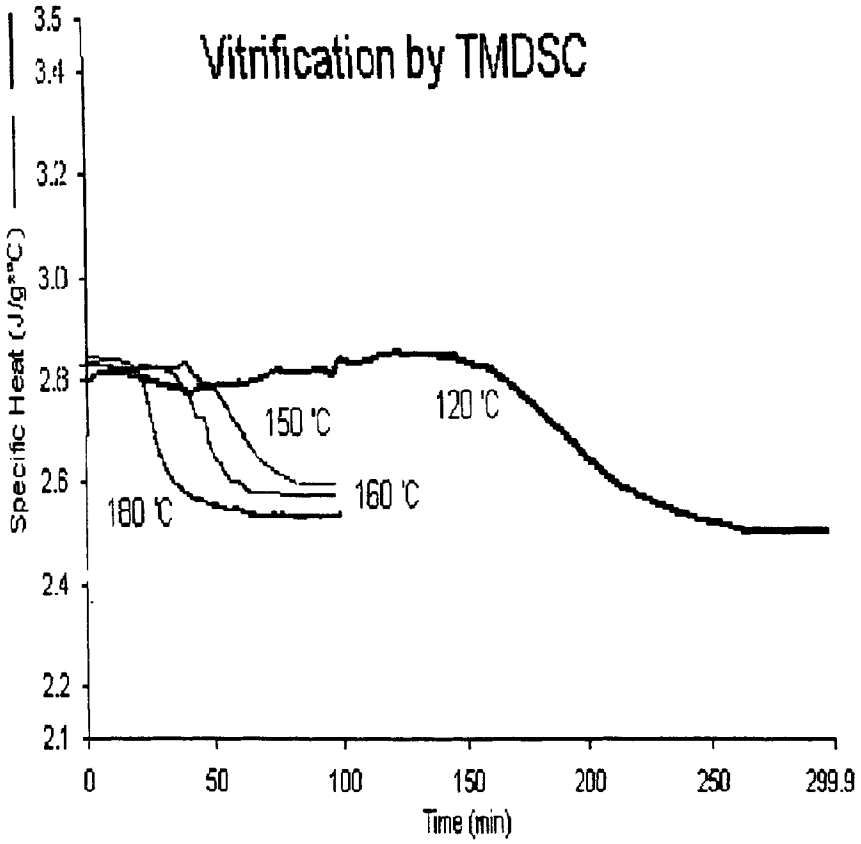

Fig. 8. Series of TMDSC isotherms with vitrification measured as the half height shifts in baseline storage C_p.

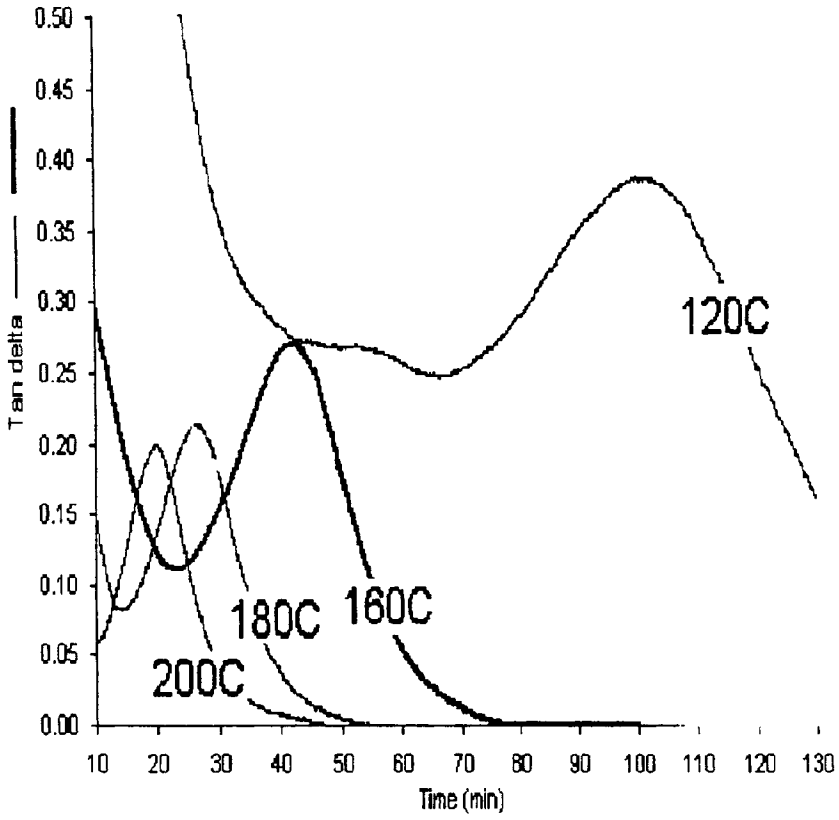

Fig. 9. A series of 3-point bending DMA isotherms showing the shift in time to vitrification for different temperatures.

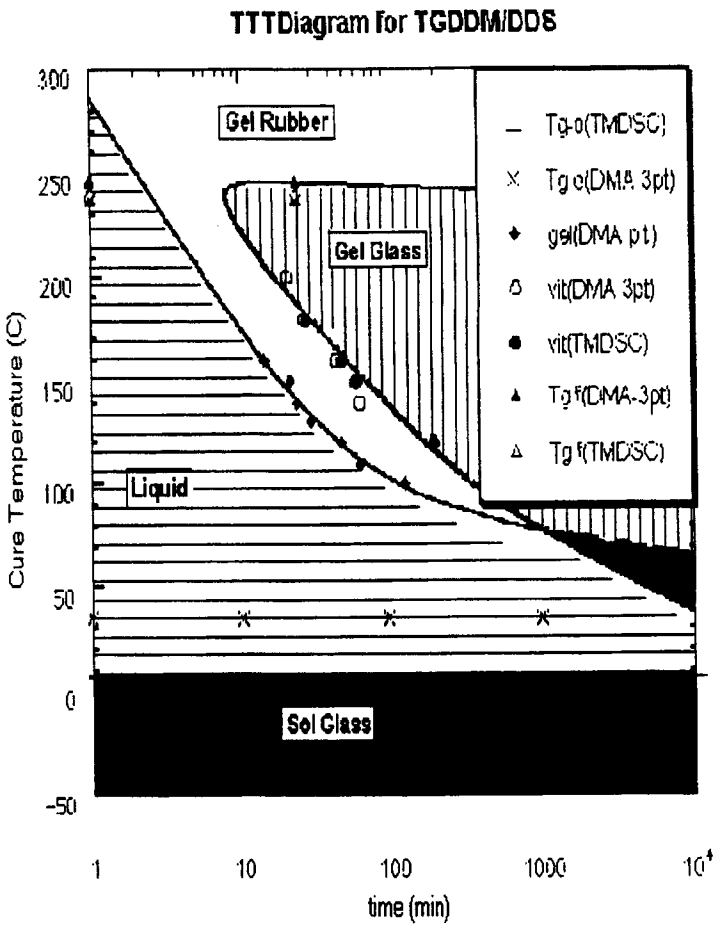

Fig. 10. Time temperature transformation diagram for the TGDDM + DDS system with gelation and vitrification curves identified. The initial T_g used for the curve was determined by DSC; however, the value from DMA 3-point bending is included as points for comparison. The gelation points were determined by DMA parallel plate measurements. The points used to construct the vitrification curve were determined by TMDSC; also here, values from DMA 3-point bending are included as experimental points for comparison. The final T_g values were determined by DMA 3-point bending and TMDSC, with DMA 3-point bending values used to construct the curve.

ACKNOWLEDGMENTS

Partial financial support has been provided by the State of Texas Advanced Research Program, Austin (project # 003594-0075) and the Robert A. Welch Foundation, Houston (grant # B-1203).

REFERENCES

1. B. Bilyeu, W. Brostow, and K. P. Menard, *J. Mater. Ed.*, **21**, 281 (1999).
2. B. Bilyeu, MS Thesis, University of North Texas, Denton (1999).
3. G. Wisanrakkit and J. K. Gillham, *Polymer Characterization*, Eds. C. Craver and T. Provder, Ch. 9, American Chemical Society, Washington D.C. (1990) 143.
4. J. M. Hutchinson and S. Montserrat, *Thermochim. Acta*, **304/305** (1997) 257.
5. J. E. K. Schawe, *Thermochim. Acta*, **270** (1995) 1.
6. J. E. K. Schawe, *Thermochim. Acta*, **261** (1995) 183.
7. J. E. K. Schawe, *Thermochim. Acta*, **260** (1995) 1.
8. K. P. Menard, *Dynamic Mechanical Analysis*, CRC Press, Boca Raton (1999).
9. M. Cassettari, G. Salvetti, E. Tombari, S. Veronesi, and G. P. Johari, *J. Polym. Sci.*, **31** (1998) 199.
10. B. Bilyeu, W. Brostow, and K. Menard, *Materials Characterization by Dynamic and Modulated Thermal Analytical Techniques, ASTM STP 1402*, American Society for Testing and Materials, West Conshocken, Pa. (2000).
11. C. Schick, J. Dobbertin, M. Potter, H. Dehne, A. Hensel, A. Wurm, A. M. Ghoneim, and S. Weyer, *J. Therm. Anal.*, **49** (1997) 499.
12. G. Van Assche, A. Van Hemelrijck, H. Rahier, and B. Van Mele, *Thermochim. Acta*, **304/305** (1997) 317.
13. J. K. Gillham, *AIChE J.*, **20** (1974) 1066.
14. H. R. O'Neal, S. Welch, J. Rogers, S. Guilford, G. Curran, and K. P. Menard, *J. Adv. Mater.*, **26** (1995) 49.
15. L. Bazyliak, M. Bratychak, and W. Brostow, *Mater. Res. Innov.*, **3** (1999) 132.
16. M. Bratychak and W. Brostow, *Polym. Eng. Sci.*, **39** (1999) 1541.
17. L. Bazyliak, M. Bratychak, and W. Brostow, *Mater. Res. Innov.*, **3** (2000) 218.